Miner Petrol (2009) 97:139–144
DOI 10.1007/s00710-009-0069-y

ORIGINAL PAPER

Evidence of weathering stages of phyllosilicates from biotite/muscovite to kaolinite, probed by EPR spectroscopy

Keller P. Nicolini · Katia C. Lombardi · Wido H. Schreiner · Irineu Mazzaro · Fernando Wypych · Antonio S. Mangrich

Received: 19 February 2009 / Accepted: 3 July 2009 / Published online: 9 August 2009

Abstract We report on a paramagnetic anisotropy study of three layered phyllosilicates. The mineral samples were characterized through X-ray powder diffraction (XRPD), X-ray photoelectron spectroscopy (XPS) and electron paramagnetic resonance (EPR). Based on EPR measurements of samples oriented parallel or perpendicular to the magnetic field lines, we show how the substitutional iron is transformed from Fe(II) (biotite) into Fe(III) (muscovite and kaolinite) species and from axial Fe(III) coordination sites (muscovite) to rhombic (kaolinite) sites in response to weathering.

Introduction

In 2002, we reported on a paramagnetic anisotropy study of a Brazilian kaolinite from the Amazon region (Schreiner et al. 2002). In kaolinite Fe(III) ions are located as substitutional impurities in octahedral sites, leading to the very uncommon anisotropy of this weak paramagnet. Recently, we described the sequestered organic matter (SOM) components separated by the same kaolinite found in the Brazilian state of Pará in the Amazon Basin, using Fe(III) impurity as a paramagnetic probe (Lombardi et al. 2006; Fukamachi et al. 2007). The mechanism for stabilizing SOM against biological attack can be improved by the presence of Al(III) cations and Al-hydroxy cations available in clay minerals. The presence of Fe(III) cations can also lead to similar effects, since these cations are both classified as hard acids (Pearson 1963) and could bind strongly to hard organic base groups like carbonylates, carboxylates and phenolates in the SOM. Kaolinite is a common 1:1 dioctahedral phyllosilicate, which is found worldwide and is especially abundant in tropical regions (Weaver 1989). This mineral has a structure composed of one silica tetrahedral sheet and one aluminum octahedral sheet. These two sheets do not match perfectly, causing a lattice distortion that occurs in both the octahedral and tetrahedral sites. Each layer is bonded to the next via Al-O-H···O-Si hydrogen bonds. Iron is the most common weathering impurity in kaolinite and is found in substitutional structural sites as well as in iron compounds adsorbed in kaolinite crystals. The magnetic properties of kaolinite and other phyllosilicates stem mainly from these iron impurities. In this study the residual Fe(III) impurity was used as a EPR probe to follow changes of Al(III) sites distortion with the weathering process. From the geological standpoint, kaolinite is the most weathered mineral of the three reported here, and its ideal formulation is $Al_2Si_2O_5(OH)_4$.

Muscovite, on the other hand, is classified as a 2:1 phyllosilicate within the mica group (Borradaile and Werner 1994). It is a widely distributed mineral found in igneous rocks, but also as a weathered decomposition of feldspars. Muscovite is a perfectly layered mineral whose ideal composition is $KAl_2(AlSi_3O_{10})(OH)_2$, and it can be

Editorial handling: A. Beran

K. P. Nicolini · F. Wypych · A. S. Mangrich (✉)
Departamento de Química, Universidade Federal do Paraná,
81531-980 Curitiba, Paraná, Brazil
e-mail: mangrich@quimica.ufpr.br

K. C. Lombardi
Departamento de Engenharia Florestal,
Universidade Estadual do Centro-Oeste,
84500-000 Irati, Paraná, Brazil

W. H. Schreiner · I. Mazzaro
Departamento de Física, Universidade Federal do Paraná,
81531-980 Curitiba, Paraná, Brazil

visualized as two tetrahedral silica sheets sandwiching an octahedral aluminum sheet. Since one of the three octahedral sites is vacant, this phyllosilicate is classified as dioctahedral. The layers by themselves are not charge-compensated, and are therefore bound ionically to each other mainly through K^+, although other ions such as Na^+ and Ca^{2+} have been found performing this bonding function. Iron can isomorphically substitute some elements of the muscovite structure, being Fe(II) ions restricted to octahedral sites.

Biotite is a dark, iron-rich 2:1 mica phyllosilicate with the general composition of $K(Mg,Fe^{2+},Fe^{3+})_3(AlSi_3O_{10})(OH)_2$. Biotite is found worldwide in granites and gneisses and its monoclinic layered crystal structure strongly resembles that of muscovite. Since the three octahedral sites in this mineral are occupied, biotite is classified as a trioctahedral phyllosilicate.

Magnetic studies of muscovite and biotite are surprisingly rare. This is probably due to the not yet found potential for possible technological applications. The discussion on the magnetic properties of phyllosilicates is concentrated mainly on geological evolutionary aspects and the study of anisotropic quantities such as magnetic susceptibility is centered on the fabric of metamorphic rocks and their strain (Borradaile and Werner 1994). Parallel to these studies and largely unrelated to them, a good amount of work has been dedicated, mainly using Mössbauer spectroscopy, to characterize Fe(II) and Fe(III) ions in phyllosillicates; their localization, their interactions, the hyperfine fields which act upon them, and the possible contamination with oxides and hydroxides (Lalonde et al. 1980; Redhammer 1998). In the eighties, Coey et al. extensively studied several rocks and minerals, and published Mössbauer as well as magnetic data on 1:1, 2:1 and 2:1:1 silicates (Coey et al. 1981; Ballet and Coey 1982; Ballet et al. 1985). They have already reported on anisotropic magnetization and susceptibility measurements, explaining their results in terms of the trigonal crystal field to which the Fe(II) ions are subjected. Beausoleil et al. (1983) reported specifically on the magnetic properties of biotite micas at low temperatures. The results were described in terms of layers having a mainly ferromagnetic order, weakly coupled antiferromagnetically to each other. The biotites of low iron content showed magnetic after effects, unstable magnetization time effects and shifted hysteresis loops, which could, according to the authors, be explained by metamagnetism or even spin-glass magnetism.

Keeping in mind the uncommon paramagnetism of kaolinite reported earlier, we extended our studies to the two other phyllosilicates, subjecting muscovite and biotite samples to several characterizations, including X-ray powder diffraction (XRPD), X-ray photoelectron spectroscopy (XPS) and electron paramagnetic resonance spectroscopy (EPR), to investigate the possible magnetic anisotropies and interactions of these layered micas.

Ionizing energetic particles resulting from nuclear decay in soils can drag out electrons from Si-O and from the Al-O bonds in kaolinite originating paramagnetic centers detected by EPR spectroscopy in the region of 3500 G, g=2 (Lombardi et al. 2002).

Experimental

PP-0559 kaolinite samples were obtained from the Rio Capim basin in the state of Pará, Brazilian Amazon region. The transparent and slightly greenish muscovite and the dark submetallic lustrous biotite samples were mined near Teófilo Otoni in the Brazilian state of Minas Gerais.

For the X-ray powder diffraction (XRPD) analysis, the solid material was placed, in the form of an oriented sample (kaolinite) or tape cleaved plaques (micas), on a glass sample holder. The kaolinite sample was oriented by suspending the powder in distilled and deionized water, dripping the suspension onto the sample holder and allowing it to dry naturally in air. All the measurements were taken with the samples oriented with the cleavage plane parallel to the sample holder which intensifies the basal diffraction peaks of the clay minerals structure. A Rigaku diffractometer with Ni-filtered CoK_α radiation (λ = 1.7902 Å) was used in the θ-2θ Bragg-Brentano geometry. All the measurements were taken using a generator voltage of 40 kV and an emission current of 20 mA. To remove undesirable fluorescent radiation, a graphite monochromator was used.

The X-ray photoelectron spectroscopy (XPS) results were obtained using a VG ESCA 3000 system with a base pressure of $2x10^{-10}$mbar. No attempt was made to remove the surface contaminants. The spectra were collected using MgK_α radiation and the overall energy resolution was approximately 0.8 eV. The energy scale was calibrated using the adventitious C_{1s} peak at 284.5 eV (Briggs and Seah 1995) as well as the Si_{2p} peak at 102.5 eV, which is the median Si_{2p} binding energy for silicates (Moulder et al. 1995; Lombardi et al. 2006). The spectra were normalized to maximum intensity.

The EPR spectra were obtained in the first derivative mode for the 5000 G range. A Bruker ESP 300E spectrometer was used in the X-band (~ 9.5 GHz) with a modulation frequency of 100 kHz, at room temperature (~ 300 K). As was done in the XRPD analysis, distilled and deionized water was used to suspend the powdery kaolinite sample by mechanical stirring. The centrifuged sample mud was dropped into the cavity of an EPR quartz biological tissue cell, left to sediment naturally and to dry in air. In the EPR spectrometer cavity, the plane of the tissue cell was

oriented parallel or perpendicularly to the magnetic field of the instrument (Lombardi et al. 2006). Being macroscopically platelet-like, the muscovite and biotite samples were measured on the plane or perpendicular to the plane in the EPR spectrometer. All the spectra were normalized for adequate comparison (Lombardi et al. 2002).

Results

Figure 1 shows the XRPD results for the three layered clay minerals. Since all the samples are oriented with their layers parallel to the sample holder, only the basal plane diffraction peaks are found. The quality of the layer packing of the micas is readily identified in the line width, and the basal plane distances of muscovite with d=9.95 Å, biotite with d=10.04 Å, and kaolinite with d=7.16 Å are highly congruent with the literature (JCPDF, ASTM Files: 14–164, 7–25 and 2–45).

The biotite sample also shows a second basal plane separation of d_B=14.0 Å. The diffraction peaks due to these planes are weak but clearly present. In Fig. 1, these diffraction peaks and their multiples are identified as B1 to B5. Biotite is known to weather in a quite peculiar fashion. Alternate layers lose their cations and expand by hydration to 14.0 Å, while the other layers remain with their original 10.04 Å separation. This interstratification of anhydrous and hydrated layers can lead to super lattice structures, which are known to display new diffraction peaks laterally to the main diffraction lines (Piecuch and Nevot 1990). The inset of Fig. 1 illustrates this phenomenon. This type of weathered biotite mica is sometimes called hydrobiotite (Velde 1992). This hypothesis was confirmed when the sample was immersed in water or magnesium chloride solution for 24 h and the intensity of the diffraction peaks increased (not shown).

The XPS measurements in Figs. 2 and 3 clearly reflect the chemical elements at the surface of the three phyllosilicates. Shown here are the survey spectra together with the identification of the elements in the main peaks.

Figure 2 shows a wide scan XPS spectrum of the biotite, muscovite and kaolinite samples. The C_{1s} peak, which is due to adventitious carbon on the kaolinite sample, was used as the binding energy reference (284.5 eV) for the spectrum (Briggs and Seah 1995). This is necessary due to sample electrical charging effects during the XPS measurements. The spectrum of biotite shows the presence of Al, Si, O, K, Mg and Fe, the muscovite spectrum shows lines

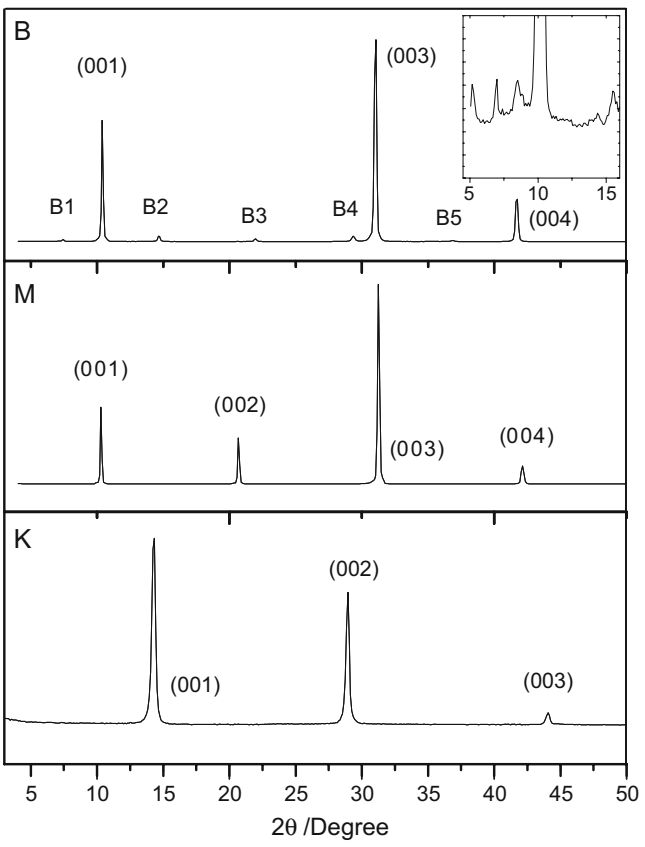

Fig. 1 X-ray powder diffraction patterns of kaolinite (K), muscovite (M) and biotite (B). The inset shows new diffraction lines due to the two distinct basal plane separations

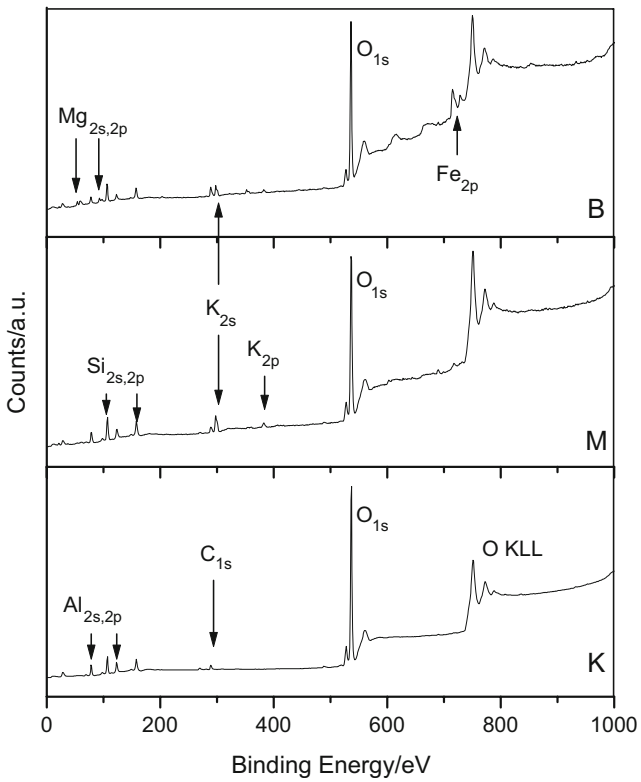

Fig. 2 XPS survey spectra of kaolinite (K), muscovite (M) and biotite (B)

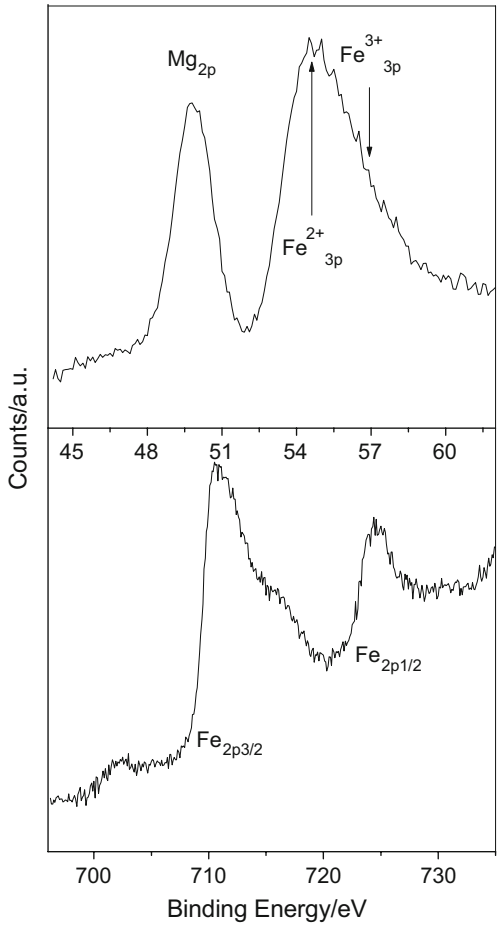

Fig. 3 Detailed XPS spectra of the Fe_{3p} and Fe_{2p} regions of biotite

for Al, Si, O and K, and the spectrum of kaolinite presents Al, Si and O as atoms of the structure constitution. The presence of the elements is consistent with the theoretical formulations of the three phyllosilicates.

As the iron content of biotite is high, a detailed spectrum of doublet Fe_{2p} (710 – 730 eV) and doublet Fe_{3p} (55 eV) were obtained (Fig. 3). The information from doublet Fe_{3p}, rather than the more intense doublet Fe_{2p} was used for the quantification of Fe(II) and Fe(III), because the peak Fe_{2p} appears in an increasing baseline showing multiple small lines. The asymmetry of the peak Fe_{3p} result from two components, Fe(II) at 54.9 eV, separated by 2.2 eV for Fe (III) at 57.1 eV. The simulation of the spectrum Fe_{3p} showed the ratio [Fe(III)/Σ (Fe(II)+Fe(III))] of 0.3. This value and the ratio [Fe/Σ(Fe+Mg)]=0.44, obtained by adjusting the curve of the spectrum, agree with other samples of biotite found in the literature. From these data it was possible to calculate the ratios Fe(II)/Fe(III)=2.3 and Mg/Fe=1.23.

Figure 4 shows the EPR spectra with magnetic fields parallel and perpendicular to the phyllosilicate planes of biotite, muscovite and kaolinite.

In spite of the relative abundance of iron in the Fe(II) oxidation state of the biotite structure, these ions are silent to EPR measurements at room temperature. Thus, the iron bivalent-rich biotite EPR spectra present only a weak isotropic line at g~4.3. This line is due to Fe(III) impurities present in small quantities in octahedral and/or tetrahedral rhombically distorted crystal sites. These iron impurities are called $Fe_{(I)}$ sites (Balan et al. 1999). As this is a magnetically isotropic site the line has about the same intensity in the parallel (∥) or perpendicular (⊥) EPR spectra (see Table 1).

The muscovite EPR spectra show several characteristic Fe(III) lines. First, there is a line at g~4.3 which is similar to but more intense than biotite in both perpendicular and parallel spectra. Then there are other lines that differ in intensity, depending on the relative orientation of the mineral sheets relative to the applied magnetic field. The perpendicular spectrum shows a broad line at $g_{\perp} \cong 6.0$ and the parallel spectrum presents a small line at $g_{\parallel} \cong 2.0$, indicating the presence of Fe(III) ions at sites with axial symmetry (Balan et al. 1999). From this observation we can conclude, following the general EPR literature, that the principal axis, i.e., the z-axis, of the octahedral tetragonally distorted (axial symmetry) Fe(III) ions is mainly parallel and that the "xy" plane is almost perpendicularly oriented in relation to the plane of the sheet of this mineral. Goodman and Hall (1994) give a detailed description of the position of the various EPR resonance lines that were calculated theoretically by Aasa (1970) (Table 1). The $g_{\perp} \cong 6.0$ line results from the transition −5/2→−3/2 in the "xy" direction, and the $g_{\parallel} \cong 2.0$ line results from the same transition −5/2 → −3/2 but now in the "z" direction (Goodman and Hall 1994). Mössbauer spectroscopy has

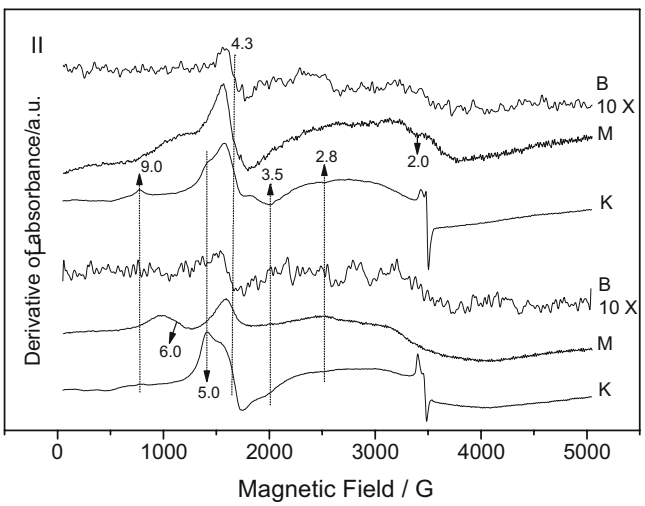

Fig. 4 Electron paramagnetic resonance spectra, parallel (∥) and perpendicular (⊥) to the mineral layers of kaolinite (K), muscovite (M) and biotite (B)

Table 1 EPR data, transition and attribution of the studied biotite, muscovite and kaolinite

Mineral	g=2	g=2	g=2.8	g=3.5	g=4.3	g=5	g=6	g=9
EPR transition	−1/2→ +1/2	−5/2→−3/2 z	−1/2→+1/2 y	−1/2→+1/2 x	−1/2→+1/2 xyz	−1/2→+1/2 z	−5/2→+3/2 xy	−5/2→-3/2 y
Attribution	Al–O Si–O	Fe(III) axial	Fe(III) ≈ axial	Fe(III) ≈ axial	Fe(III) rhmb.	Fe(III) ≈ axial	Fe(III) ≈ axial	Fe(III) rhmb.
(∥) spectra								
Biotite	No	No	No	No	Yes S	No	No	No
Muscovite	No	Yes W	No	No	Yes S	No	No	No
Kaolinite	Yes S	No	Yes W	Yes S	Yes S	Yes W	No	Yes S
(⊥) spectra								
Biotite	No	No	No	No	Yes S	No	No	No
Muscovite	No	No	No	No	Yes S	No	Yes S	No
Kaolinite	Yes S	No	No	Yes W	Yes S	Yes S	No	No

Al–O, Si–O=paramagnetic centers; ≈axial=almost axial sites; (∥)=parallel spectra; (⊥) = perpendicular spectra; S=strong; W=weak. Rhmb=rhombic

shown that Fe(III) and Fe(II) ions occur exclusively in octahedral sites (Mydosh 1993).

However, this observation is not applicable to kaolinite. The levels of isomorphous substitutions of iron for aluminum in the kaolinites are usually low, and substitution of Fe for Si in tetrahedral sites is generally believed not to occur (Aasa 1970). This mineral presents residual Fe(III) ions in two kinds of sites: $Fe_{(I)}$ in rhombically distorted sites with g ≅ 4.3 like the micas, and $Fe_{(II)}$ with a more axial structure but less symmetrical than that of the muscovite mineral. This $Fe_{(II)}$ center presents preferential orientations regarding the layer planes. This anisotropy can be clearly identified, since the g=9.0, 3.5 and 2.8 lines are enhanced in the parallel EPR spectrum, while the g=5.0 line is intensified for the perpendicular spectrum. The g= 9.0, 5.0, 4.3, 3.5 and 2.8 lines result from the −5/2 → −3/2 "y", −1/2 → +1/2 "z", −1/2 → +1/2 "xyz", −1/2 → +1/2 "x" and −1/2 → +1/2 "y" electronic spin transitions, respectively (Balan et al. 1999; Lombardi et al. 2002). Thus, the spectra show that the "z" axis of this Fe(III) center has a preferred perpendicular orientation to the kaolinite layers.

Discussion and conclusions

The XRPD and XPS results clearly characterize the samples of muscovite, biotite and kaolinite and are useful in showing congruence with the literature. Biotite shows two basal plane separations, indicating that part of the K^+ ions intercalated between the mica layers are partially hydrated.

This distinct behavior can also be seen in our anisotropic EPR measurements of muscovite compared to kaolinite. Fe (III) ions, which reside only in octahedral sites in both minerals, display different resonant EPR transitions and depend anisotropically on the direction of the applied magnetic field relative to the mineral layers. As described above, the "z"-axis of the Fe(III) impurities in octahedral sites seems to be parallel or nearly parallel to the muscovite mica layers and perpendicular or almost perpendicular to the kaolinite layers. The EPR measurements probe Fe(III)-related anisotropies with respect to in-plane and out-of-plane measurements. The octahedral sites in the micas reside in a quite different environment than that of kaolinite. While the octahedral sites in kaolinite at one side are adjacent to hydroxyl groups, which are bound by hydrogen bonds to the next silicate sheet, the octahedral sites in the micas are located between the apical oxygens of two silicate sheets. This different environment of the octahedral sites leads to different lattice distortions and to different crystal fields that act on the iron impurities. The joint action of crystal fields and applied magnetic fields should explain the dissimilar anisotropies found in these layered minerals, which seem to constitute a fine test bed for further fundamental studies. EPR studies show that the weathering from biotite to kaolinite, through muscovite, corresponds to varying the Fe(III) site symmetry from a residual rhombic structure in biotite, to rhombic and axial symmetries in muscovite until a rhombic and a more symmetrical site (but not yet totally axial as in muscovite) is obtained in kaolinite.

Acknowledgements The authors thank the Brazilian agencies CAPES, CNPq, PRONEX and FINEP for their financial support. We are especially indebted to Prof. Eleonora M. Gouvêa (Geology Department of the Federal University of Paraná) for providing the mica samples.

References

Aasa R (1970) Powder line shapes in the electron paramagnetic resonance spectra of high-spin ferric complexes. J Chem Phys 52:3919–3930

Balan E, Allard Th, Boizot B, Morin G, Muller AP (1999) Structural Fe^{3+} in natural kaolinites: new insights from EPR spectra fitting at X- and Q-band frequencies. Clays Clay Miner 47(5):605–616

Ballet O, Coey JMD (1982) Magnetic properties of sheet silicates; 2:1 layer minerals. Phys Chem Miner 8:218–229

Ballet O, Coey JMD, Burke KJ (1985) Magnetic properties of sheet silicates; 2:1:1 layer minerals. Phys Chem Miner 12(6):370–378

Beausoleil NP, Lavallee A, Yelon O, Ballet O, Coey JMD (1983) Magnetic properties of micas. J Appl Phys 54:906–915

Borradaile G, Werner T (1994) Magnetic anisotropy of some phyllosilicates. Tectonophys 235:223–248

Briggs D, Seah MP (1995) Practical surface analysis by Auger and X-ray-photoelectron-spectroscopy. Wiley, Chichester

Coey JMD, Ballet O, Moukarika A, Soubeyroux JL (1981) Magnetic properties of sheet silicates: 1:1 layer minerals. Phys Chem Miner 7:141–148

Fukamachi CRB, Wypych F, Mangrich AS (2007) Use of Fe^{3+} ion probe to study the stability of urea-intercalated kaolinite. J Colloid Interface Sci 313:537–541

Goodman BA, Hall PL (1994) Electron paramagnetic resonance spectroscopy. In: Wilson MJ (ed) Clay mineralogy: spectroscopic and chemical determinative methods. Chapman & Hall, London

JCPDF: Joint Committee on Powder Diffr. Files. Am. Soc. for Testing of Materials - ASTM - Files: 14−164, 7−25 and 2−45, 2001

Lalonde AE, Rancourt DG, Ping JY (1980) Accuracy of ferric/ferrous determinations in micas: a comparison of Mössbauer spectroscopy and the Pratt and Wilson wet-chemical methods. Hyerfine Interact 117:175–204

Lombardi KC, Guimarães JL, Mangrich AS, Mattoso N, Abbate M, Schreiner WH, Wypych F (2002) Structural and morphological characterization of the PP-0559 Kaolinite from the Brazilian Amazon region. J Braz Chem Soc 13(2):270–275

Lombardi KC, Mangrich AS, Wypych F, Rodrigues-Filho UP, Guimarães JL, Schreiner WH (2006) Sequestered carbon on clay mineral probed by electron paramagnetic resonance and X-ray photoelectron spectroscopy. J Colloid Interface Sci 295:135–140

Moulder JF, Stickle WF, Sobol PE, Bomben KD (1995) Handbook of X-ray photoelectron spectroscopy. Physical Electronics INC. Eds, Eden Prairie, USA, In

Mydosh JA (1993) Spin glasses: an experimental introduction. Taylor and Francis, London

Pearson RG (1963) Hard and soft acids and bases. J Amer Chem Soc 85:3533–3539

Piecuch M, Nevot L (1990) X-ray and neutron characterization of multilayer systems. In: Chamberod A, Hillairet J (eds) Metallic multilayers: materials science forum, vol 59 & 60. Trans Tech Publ, Switzerland

Redhammer GJJ (1998) Characterization of synthetic trioctahedral micas by Mossbauer spectroscopy. Hyp Interact 117:85–115

Schreiner WH, Lombardi KC, De Oliveira AJA, Mattoso N, Abbate M, Wypych F, Mangrich AS (2002) Paramagnetic anisotropy of a natural kaolinite and its modification by chemical reduction. J Magn Mag Mat 241:422–429

Velde B (1992) Introduction to clay minerals. Chapman & Hall, Cambridge

Weaver CE (1989) Clays, muds and shales: developments in sedimentology. Elsevier, Amsterdam